Frontiers in Bioscience Landmark

Front. Biosci. (Landmark Ed) **2026**; 31(7): 53279
https://doi.org/10.31083/FBL53279

Original Research

Peripheral Administration of isoD7-Aβ Exacerbates Motor Deficits and Tau Pathology in P301S Mice

Yulia Stepenko[1,*], Olesya Shcheblykina[1], Nikita Zhunusov[1], Veronika Shmigerova[1], Sergey Kozin[2], Vladimir Mitkevich[2], Alexandra Radchenko[1], Elena Kuzubova[1], Leonid Khalzov[3], Mikhail Korokin[1]

[1]Department of Pharmacology and Clinical Pharmacology, Belgorod State National Research University, 308015 Belgorod, Russia
[2]Laboratory of Protein Conformational Polymorphism in Health and Disease, V.A. Engelhardt Institute of Molecular Biology, Russian Academy of Sciences, 119991 Moscow, Russia
[3]Faculty of Fundamental Medicine, Pavlov First Saint Petersburg State Medical University, 197022 Saint Petersburg, Russia
*Correspondence: stepenko@bsuedu.ru (Yulia Stepenko)
Academic Editor: Katsuhiko Tabuchi
Submitted: 24 April 2026 Revised: 16 June 2026 Accepted: 23 June 2026 Published: 24 July 2026

Abstract

Background: Alzheimer's disease (AD) is a progressive neurodegenerative disorder leading to dementia, disability, and premature death. Beta-amyloid (Aβ) and tau pathology are considered key components of its pathogenesis; however, the role of peripheral amyloid load in modulating pre-existing tau pathology remains understudied. We hypothesized that peripheral amyloid load could exacerbate tau pathology through mechanisms potentially linked to the disruption of the Akt/glycogen synthase kinase-3β-associated signaling pathway, which could lead to increased behavioral deficits and progression of neurodegenerative changes. **Objective:** To evaluate the effect of double peripheral (retro-orbital) administration of the Aβ isoform D7 on the behavioral phenotype, morphological signs of tau pathology, and the expression of genes related to Akt/GSK-3β-associated signaling, neuroinflammation, and apoptosis in the brains of P301S transgenic mice. **Materials and Methods:** The study included 12-week-old male P301S transgenic mice (Tg(Thy1-MAPT*P301S)2541Godt) (n = 20, biological duplication) and wild-type C57Black6/J mice (n = 10). P301S mice received two retro-orbital injections of isoD7-Aβ into the venous sinus at a dose of 100 µg (n = 10) with a 1-month interval; control P301S mice received an equivalent volume of water for injection (n = 10). Behavioral testing ("open field", "novel object recognition", "vertical pole", "inverted screen") was performed at 16 and 20 weeks of age. Tau pathology was assessed immunohistochemically using AT-8 (pSer202/pThr205) antibodies in the frontal cortex and brainstem, and amyloid deposits were assessed histologically using Congo red staining in the entorhinal cortex and hippocampus. The expression of *Akt1, Gfap, Mapt, Cdk5, Casp3, Bax*, and *Bcl2* genes in brain tissue was analyzed by quantitative real-time PCR. **Results:** Two peripheral administrations of isoD7-Aβ were not associated with further deterioration of performance in the "open field" and "novel object recognition" tests compared to the control P301S group, which likely reflects the already established deficit characteristic of this transgenic line. In contrast, in motor coordination tests ("vertical pole", "inverted screen"), motor impairments in the P301S+Aβ group emerged by week 16, whereas in P301S mice without amyloid load, they appeared only by week 20. Immunohistochemical analysis revealed an increase in AT-8-positive staining in the brainstem, whereas no statistically significant differences were found between groups in the frontal cortex. Histological analysis did not reveal amyloid plaques in the entorhinal cortex and hippocampus of P301S+Aβ mice and control P301S mice. At the molecular level, the P301S+Aβ group showed decreased Akt1 expression, increased Gfap and Bax expression, and decreased Bcl2 expression, with no significant changes in Mapt, Casp3, and Cdk5. This pattern is consistent with dysregulation of Akt/GSK-3β-associated signaling, enhanced glial activation, and a pro-apoptotic shift. **Conclusions:** Two peripheral administrations of isoD7-Aβ to P301S mice were associated with earlier development of motor impairments, increased tau protein phosphorylation, and changes in gene expression consistent with a disrupted Akt/GSK-3β-associated signaling pathway. These findings support the hypothesis that peripheral amyloid load can exacerbate tauopathy manifestations, and the observed transcriptional changes are consistent with the possible involvement of the Akt/GSK-3β-associated signaling pathway, which may represent a potential therapeutic target in AD.

Keywords: Alzheimer's disease; amyloid beta-peptides; tau proteins; protein phosphorylation; mice, transgenic

1. Introduction

According to current estimates, the number of people suffering from neurodegenerative diseases continues to grow steadily, reaching approximately 50 million worldwide [1]. Alzheimer's disease (AD) is one of the major medical and social challenges worldwide [2]. Despite years of research, options for disease-modifying therapy in AD remain limited, and available clinical care largely retains a symptomatic nature. In this regard, the search for new pathogenetically justified approaches to the therapy and prevention of AD remains an extremely urgent task [3].

For a long time, the "amyloid hypothesis" dominated the scientific community, according to which the main trigger mechanism of AD is the accumulation of beta-amyloid (Aβ) in brain tissue — a peptide generated by proteolytic processing of amyloid precursor protein (APP). The accumulation of toxic Aβ oligomers and fibrils was considered the primary cause of synaptic dysfunction and neuronal death [4,5]. Despite a prolonged period of ambiguous results in clinical trials of anti-amyloid drugs, in recent years, monoclonal antibodies against Aβ have been introduced into clinical practice, capable of slowing the clinical progression of Alzheimer's disease in its early stages. However, their clinical effect remains moderate, and their use is limited by several patient selection criteria and risks, including amyloid-related imaging abnormalities (ARIA). This indicates that the amyloid component of pathogenesis is of fundamental importance, but it does not exhaust all mechanisms of disease progression, including those associated with tau pathology [6,7,8].

Currently, a significant amount of data has been accumulated indicating the critical role of another pathological protein — tau. In AD, tau protein undergoes post-translational modifications, forming intracellular neurofibrillary tangles, which ultimately lead to microtubule destabilization, disruption of intracellular transport, and neuronal death. In this regard, one of the key questions in the pathogenesis of AD remains the mechanism of interaction between extracellular Aβ and intracellular tau pathology. Modern research shows that Aβ oligomers can indirectly trigger the cascade of pathological tau protein phosphorylation by activating specific kinases, including GSK-3β [9,10,11]. Thus, a complex pathogenetic interaction is formed, in which Aβ acts as a trigger, and tau pathology acts as a direct effector of neurodegeneration.

However, the role of peripheral Aβ signaling in modulating pre-existing tau pathology has been insufficiently studied. Of particular interest are not native forms of Aβ, but its post-translationally modified variants, specifically Aβ with an isomerized aspartic acid residue at position 7 (isoD7-Aβ, isoAβ42) (Fig. 1). It has been shown that isoAβ42 is one of the most common isoforms of Aβ in amyloid plaques and possesses more pronounced neurotoxic properties compared to intact Aβ42 [12,13]. In SH-SY5Y neuroblastoma cells, the introduction of synthetic isoAβ42, unlike native Aβ42, was accompanied by a significantly higher level of protein phosphorylation, particularly of tau protein, tubulins, and matrin 3, indicating the ability of this isoform to trigger pathological processes associated with tau dysregulation [14]. These findings formed the basis for choosing isoD7-Aβ as the experimental agent in the present study.

The aim of the study was to evaluate the effect of peripheral systemic administration of isomerized beta-amyloid — a synthetic analogue of human Aβ, isomerized at the aspartic acid residue at position 7 (isoD7-Aβ) — on the behavioral phenotype, morphological features of tau pathology, and the expression of genes associated with the Akt/GSK-3β-associated signaling pathway, neuroinflammation, and apoptosis in brain tissue of P301S transgenic mice.

2. Materials and Methods

Three groups of 12-week-old male mice were included in the study: the wild-type control group (C57Black6/J, n = 10, biological duplication), which received 100 micrograms of phosphate-buffered saline (PBS) into the retroorbital venous plexus twice with an interval of 1 month; the P301S control group, which received 100 micrograms of PBS into the retroorbital venous plexus twice with an interval of 1 month (n = 10), and the P301S + isoD7-Aβ group, which received two retroorbital injections of isoD7-Aβ (100 micrograms per injection, n = 10) with an interval of 1 month. The animals and synthetic isoD7-Aβ peptide were provided by the Laboratory of Modeling Neurodegenerative Processes, Institute of Physiologically Active Substances, Russian Academy of Sciences (Chernogolovka). The animals were housed in the experimental-biological clinic with SPF status (vivarium) of Belgorod State National Research University (BelSU).

Animals were allocated to groups using simple randomization. The animal housing conditions were in accordance with the current sanitary rules for the design, equipment, and maintenance of experimental biological clinics. The animals were kept in groups of 10 per cage at a temperature of 20–22 ℃, humidity of 45–65%, with a constant supply of water and food, and 12 hours of daylight (from 8 a.m. to 8 p.m.). Laboratory animals with a "specific pathogen-free" (SPF) status were obtained from the Research Institute of Pharmacology of Living Systems.

Inclusion: Male P301S and C57Black6/J mice, 12 weeks old at the start of the experiment, with no visible signs of disease, obtained from the same laboratory (IPAV RAS). Exclusion: Animals with visible signs of disease. Data point exclusion: None.

Animals from the corresponding group were euthanized at 24 weeks of age. These animals were deeply anesthetized by intraperitoneal administration of 10% Zoletil 100 (containing 50 mg/mL tiletamine and 50 mg/mL zolazepam, Virbac, France) at a dose of 30 mg/kg in combi-

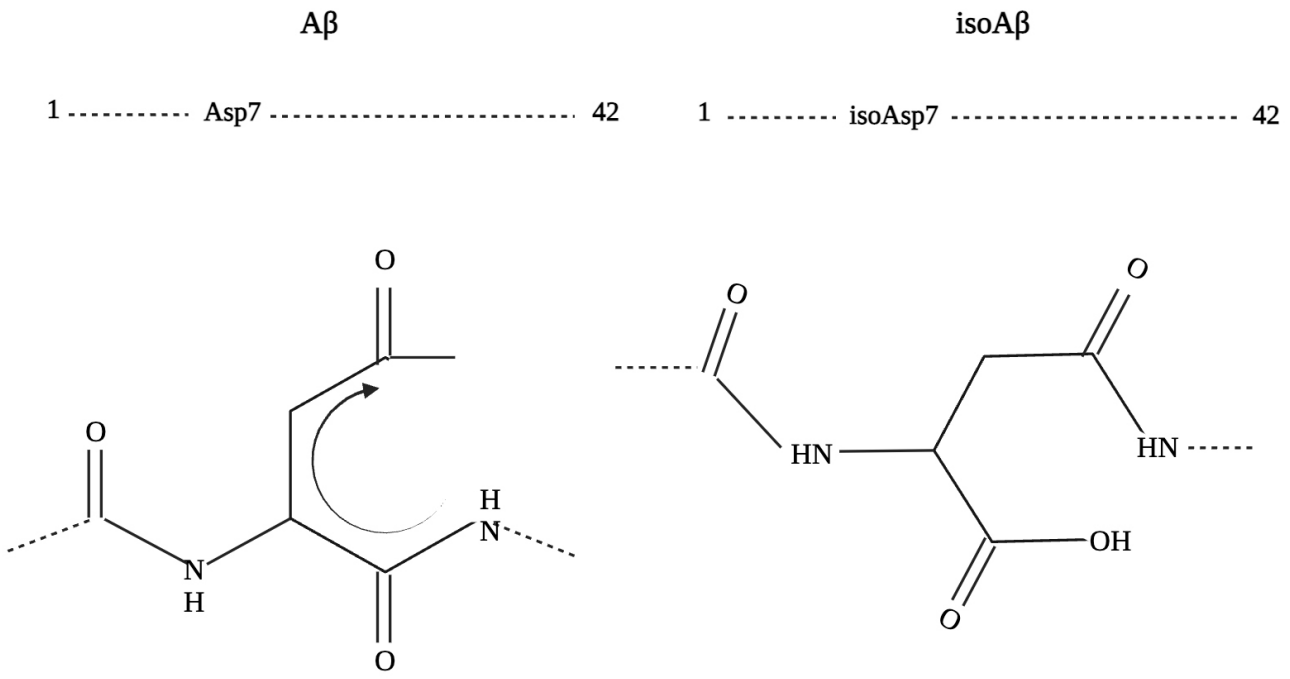

Fig. 1. Spontaneous isomerization of Asp7 in beta-amyloid forms a succinimide intermediate; its hydrolysis yields L-isoaspartate (isoAsp), altering the main-chain conformation. The resulting new peptide bond alters the conformation of the main chain.

nation with 2% xylazine solution (20 mg/mL, Biogel, Belarus) at a dose of 12 mg/kg and achievement of the surgical stage of anesthesia (absence of the root reflex and the state of pinching of fingers/tail), intracardiac administration of 2% lidocaine hydrochloride solution (Grotex, Russia) at a dose sufficient (4 mg/kg) to achieve immediate cardiac arrest.

2.1 Peptide Preparation and Administration Scheme

Specially lyophilized isoD7-Aβ peptide was dissolved in sterile water and the pH of the solution was adjusted to neutral using NaOH. The resulting solution was further diluted with sterile phosphate-buffered saline (PBS) to a final peptide concentration of 1 mg/mL, and then sterilized by steam in an autoclave at 112 °C for 10 minutes. The initial sterile peptide solutions, intended for all subsequent experiments, were prepared simultaneously according to a single protocol and stored in aliquots of 0.5 ml at –20 °C for 1–8 months.

An additional limitation of the study is that we did not directly assess the structural stability or aggregation state of isoD7-Aβ after autoclave sterilization. Therefore, although the preparation protocol was based on a previously published *in vivo* approach, the isoD7-Aβ peptide has a special thermal stability under these conditions (112 °C, 10 min is a relatively mild regime compared to 121 °C or prolonged heating). The key difference in the literature is shown due to the degradation of mature amyloid fibrils when heated. In our case, the peptide was in an oligomeric state (freshly dissolved) before sterilization, and not in the form of mature fibrils. The aggregation process is induced after sterilization (during storage and/or administration). The thioflavin *T* test is a standard and sensitive method, and if the thioflavin T fluorescence in the sterilized samples did not differ from the control, this is evidence of the absence of changes in β-amyloid-containing structures in the results of S.Kumar et al. 2011 [15]. Reproducibility over time (1–8 months of storage) additionally confirms that sterilization did not create “incorrect” aggregates unstable during storage, since the results of H.Fukuda et al. 1999 provide a valid justification that the isomeric form (isoD7) does not change the aggregation ability [14,15,16].

Immediately before administration, an aliquot of the stock solution was diluted with sterile physiological saline to a concentration of 500 μg/mL. Each injection sample was prepared immediately before administration to the animals.

The retro-orbital route of administration was chosen as a minimally invasive method for systemic delivery of substances with rapid entry into the bloodstream, widely used in mouse experiments. The administration was performed twice with a 1-month interval between injections.

Intravenous injection into the retroorbital venous plexus in mice is allowed in the absence of anesthesia. To perform this procedure, the mouse is grabbed by the skin of the neck with the thumb and forefinger, the other fingers are securely held by the skin of the back and pressed against the mesh for maintenance. The conjunctiva of the inner corner of the eye is pierced with a syringe needle and held to a depth of 1–2 mm behind the eyeball, where the venous plexus is located. When properly inserted into the

needle, blood flows by gravity from the retroorbital plexus (if in doubt, a slight negative pressure can be created in the syringe). After making sure that the location is correct, the test drug is slowly injected. After injection, the eyeball is lightly pressed with a sterile gauze cloth to stop the bleeding. In this way, the drug can be administered with a syringe with a volume of 1 ml and a needle No. 27-29G½. The volume of the injected drug is 200 μL/head. Throughout the experiment, mice are kept individually in cages.

2.2 Behavioral Activity Assessment

2.2.1 Open Field Test

This testing protocol is designed to quantitatively assess rodent behavioral activity, including exploratory and locomotor activity. The assessment parameters include: movement speed, total distance traveled, and time spent in the central and peripheral zones of the experimental arena. The study was conducted using an open arena (OpenScience, Russia) measuring 50 × 50 cm with 40 cm high walls. The experimental field was uniformly illuminated (40 lux). Animal movements were recorded using a video camera positioned above the arena. The duration of each test session was 5 minutes.

2.2.2 Novel Object Recognition Test

This test is designed to assess the selective exploratory activity of mice, i.e., their tendency to preferentially interact with a novel object compared to a familiar one. The study protocol included three stages:

1. Acclimation Stage: Animals freely explored the experimental arena (open field, white box measuring 40 × 40 × 40 cm) without any objects. Upon completion of this stage, the animal was temporarily removed from the arena and placed in an individual cage.

2. Familiarization Stage (or Exposure): During a set period, each mouse was placed in the arena with two identical objects. The duration of this stage was 5 minutes, after which the animal was returned to its cage.

3. Testing Stage (Memory Recognition): 24 hours after the familiarization stage, the ability to recognize was assessed. The animal was placed in the arena where one familiar object (from the previous exposure) and one novel object were present. The obtained results regarding the total distance and speed of the animals, preference indices, discrimination indices, and an indicator of interest in the novel object were then analyzed to further evaluate the mice's learning and memory abilities.

Preference index RI = Tn/(T1 + T2 + Tn + T_f), normalization: the preference index ranges from –1 to +1. A value of 0 means equal time spent with new and familiar objects. A positive value indicates a preference for a new object, a negative value indicates a preference for a familiar one.

Discrimination index DI = (Tn – T_f)/(T1 + T2 + Tn + T_f),

where:

Tn is the time of studying a new object;

T_f — time to explore a familiar object;

T1 and T2 are the time spent exploring the original objects.

Normalization: The discrimination index also varies from –1 to +1. A positive value indicates more time spent with a new object, a negative value indicates time spent with a familiar object, and 0 means no preference.

Statistical basis of comparison: Analysis of variance (ANOVA), Post-hoc tests.

The movements of the animals were recorded using a video camera located above the arena and analyzed using the tracking software Noldus Ethovision XT (Noldus Information Technology, Leesburg, Virginia). The following parameters were analyzed: the total distance traveled, the average speed, the number of visits to the center and to the periphery, as well as the time spent in the central and peripheral zones.

2.2.3 Vertical Pole Test

This test is necessary to assess motor coordination and balance in animals. The trial involved determining the time for the animal to turn on a vertical pole and the maximum time the animal could remain on the vertical pole. The apparatus consisted of a metal pole with a diameter of 1 cm and a length of 50 cm. The animal was placed on the upper part of the pole with its hind paws on its surface and its front paws on the lid. The duration of each trial was 60 seconds, and the time spent on the pole was recorded. A total of three independent trials were conducted for each animal with 5-minute intervals between them.

2.2.4 Inverted Screen Test

This test is necessary to assess the motor activity and endurance of animals. The animal is placed on a rectangular wire mesh with a 0.5 cm spacing between wires, and the mesh is inverted. The mouse hangs, clinging to the wires of the mesh for 3 minutes. If the mouse falls, it has 2 more attempts, and the value with the shortest retention time on the inverted mesh wire is recorded.

All behavioral test results were statistically analyzed using GraphPad Prism 8.0 software (Version number 8.0, San Diego, CA, USA). For the analysis of behavioral test data, a two-way analysis of variance (ANOVA) with factors "group" and "testin "gage" where "testing age" referred to the two behavioral assessment time points (16 and 20 weeks) was used, followed by Tukey's post-hoc test. The normality of distribution was assessed using the Shapiro-Wilk test. Values were considered statistically significant at $p < 0.05$.

2.2.5 Immunohistochemical and Histological Assessment of Brain Structures

Animals from the studied groups at the age of 24 weeks were euthanized by intracardiac injection of 2% lidocaine hydrochloride (Grothex, Russia) after intraperitoneal anesthesia with Zoletil 100 (Virbac, France) at a dose of 30 mg/kg in combination with xylazine (Biogel, Belarus) at a dose of 12 mg/kg. Following this, tissue dissection was performed.

Immediately after anesthesia, perfusion with chilled PBS solution was carried out to remove blood from the brain vessels and cool the tissue. The brain was rapidly dissected on ice. The right hemisphere, obtained by dissection, was fixed in Bouin's solution (71.4% saturated picric acid, 23.8% formaldehyde, 4.8% glacial acetic acid), after which frontal sections were prepared using a vibratome (Leica Microsystems GmbH).

A portion of the paraffinized sections was deparaffinized and washed in EnVision Flex buffer (1:1000 dilution) in two containers for 3 minutes. Then, the sections were treated in Trilogy™ citrate buffer (25:500 dilution) at 100 °C for 1 hour, cooled for 20 minutes, and repeatedly washed in washing buffer and distilled water for 3 minutes in two containers. Immunohistochemical staining was performed using AT-8 monoclonal antibodies (1:1000 dilution). After this, the sections were again washed in washing buffer and distilled water for 5 minutes. Subsequently, a two-component HiDef Detection™ system was applied: first, incubation with the detection reagent for primary mouse and rabbit antibodies for 10 minutes, then with HRP-conjugated horseradish peroxidase for 15 minutes at room temperature. The reaction was visualized using DAB Chromogen + DAB Buffer for 1 minute. The sections were counterstained with Mayer's hematoxylin for 2 minutes, dehydrated in 100% isopropanol in three containers for 3 minutes, then cleared in orthoxylene in four containers for 3 minutes. After this, the specimens were mounted under coverslips using Vitrogel mounting medium.

The second portion of the paraffinized sections was used for Congo Red staining. The sections were deparaffinized in xylene for 20 minutes, then rehydrated by sequential incubation in ethanol solutions: 10 minutes in 100%, 5 minutes in 95%, and 5 minutes in 50%, after which they were washed three times in distilled water for 5 minutes each. Next, the sections were stained with a 0.5% Congo Red solution in 50% ethanol for 5 minutes and differentiated in a 0.2% potassium hydroxide solution in 80% ethanol for 1 minute. After three washes in distilled water for 5 minutes each, the specimens were mounted under coverslips using Glasseal mounting medium (Labico LLC, Russia) (Fig. 2).

2.3 Morphometric Analysis

The prepared slides were analyzed using a Nikon Eclipse Ts2R microscope (Amstelveen, the Netherlands) equipped with a motorized stand. Panoramic visualization of mouse brain slices in the TRITC fluorescent mode was performed using a 10× lens using NIS Elements AR software (version 4.6, Laboratory Imaging, Prague, Czech Republic) with combining frames into a single composite image, overlapping 10% and automatic post-processing. To determine AT-8 -immunostained neurons in the frontal cortex (5300 μm^2) and brainstem (2300 μm^2), counting was performed manually. To determine Congo red-positive amyloid deposits, counting was performed manually based on a threshold brightness value relative to the baseline brightness of amyloid deposits in intact brain tissue. Morphometric data were expressed as a percentage of the Congo red-positive deposit area within the studied region. Morphometric data were expressed in % as a fraction of the area of Congo red-positive deposits in the study area.

2.4 Relative Normalized Gene Expression Analysis

The frontal cortex of the left hemisphere of the brain was used as the material for quantitative gene expression analysis. After isolation, it was immediately snap-frozen in liquid nitrogen.

Total RNA isolation was performed using the RNeasy Kit (Qiagen, Germany) according to the manufacturer's instructions. The RNA concentration at the output was measured spectrophotometrically with a NanoDrop OneC instrument (Thermo Scientific, USA). 1 µg of total RNA was used for the reverse transcription reaction using the MMLV RT kit (Evrogen, Russia). The temperature protocol was: 40 °C – 60 min, 70 °C – 10 min. After cDNA synthesis, samples were immediately placed on ice and subsequently subjected to analysis.

For qPCR, a ready-made mixture of 5× qPCRmix-HS SYBR (Evrogen, Russia) with the intercalating dye Sybr Green I was used. Primers for genes of interest (GOI) were designed to allow simultaneous amplification under the same temperature conditions along with a housekeeping gene (HKG) (Table 1). Each sample was added to the plate in three replicates, the results of which were averaged for further calculations. Amplification was performed using a CFX96 Touch Real-Time PCR Detection System (Bio-Rad Laboratories Inc., USA) according to a two-step thermal protocol: (1) initial denaturation — 95 °C, 300 s; (2) cycling denaturation — 95 °C, 5 s; (3) annealing+elongation — 60 °C, 30 s; number of cycles 45. The specificity of the reaction products was controlled by analysis of melting curves (MCA): 65 °C –90 °C over 25 minutes with a step of 0.5 °C.

The results of the PCR analysis were expressed using the formula $2^{-\Delta Ct}$, where $\Delta Ct = Ct(GOI) - Ct(Gapdh)$.

3. Results

3.1 Behavioral Testing Results

In the "Open Field" test, the P301S+Aβ group generally did not show further deterioration of performance

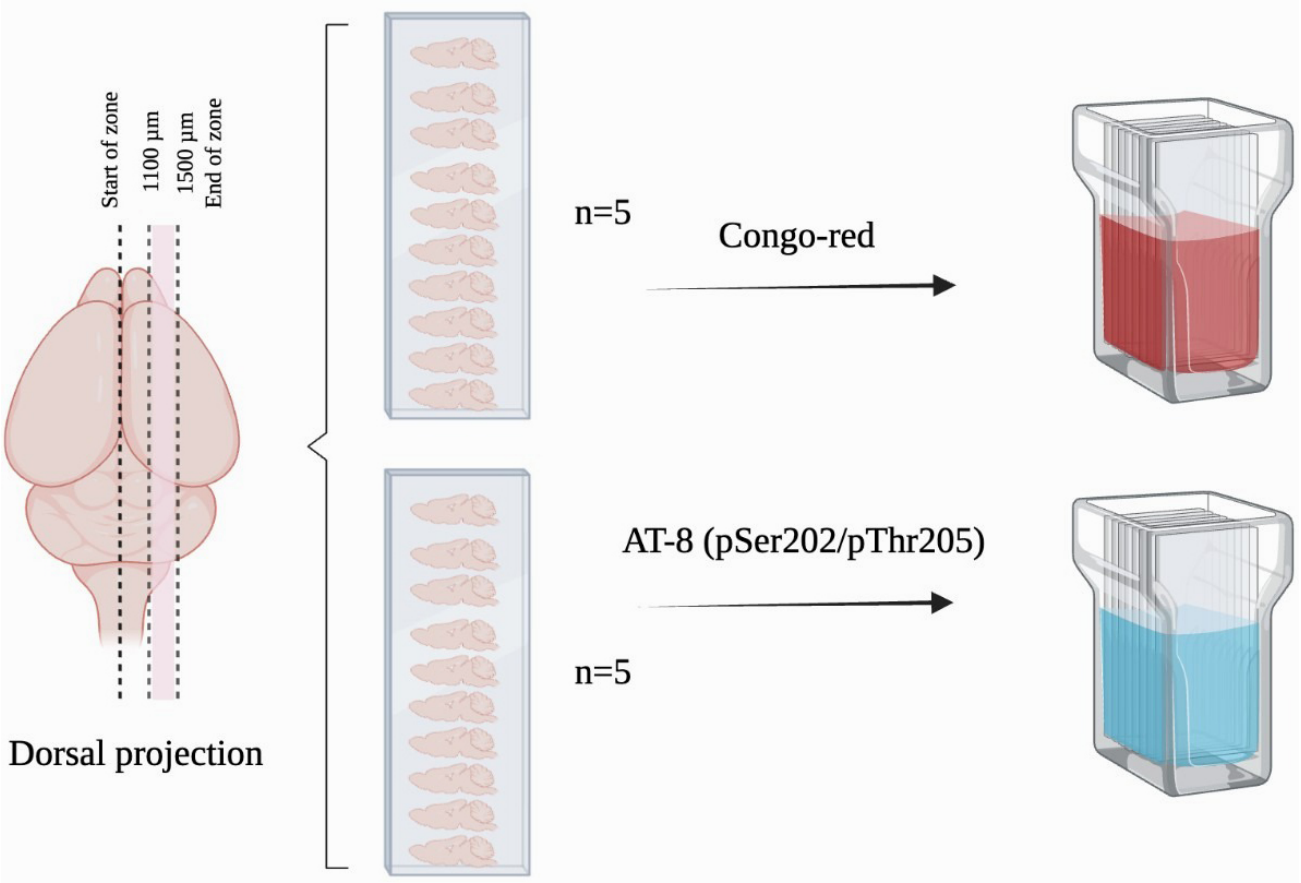

Fig. 2. Diagram illustrating the arrangement of brain sections during the preparation of immunohistochemical and histological samples. From the right cerebral hemisphere, 5 slides were prepared, the thickness of each slice is 400 µm, with each slide consisting of 10 brain sections; every fifth brain section was placed on each slide. Created in BioRender. Pokrovkiy, V. (2026) https://BioRender.com/atyhot0.

Table 1. Oligonucleotide sequences for PCR analysis.

Genes	Forward primer	Reverse primer
Akt1	5′-AAGGACCCTACACAGAGGCT-3′	5′-AAGGTGGGCTCAGCTTCTTC-3′
Gfap	5′-ACAGAGGAGTGGTATCGGTCT-3′	5′-GCGGCGATAGTCGTTAGCTT-3′
Casp3	5′-AGCTTGGAACGGTACGCTAA-3′	5′-GAGTCCACTGACTTGCTCCC-3′
Bax	5′-CTACAGGGTTTCATCCAG-3′	5′-CCAGTTCATCTCCAATTCG-3′
Bcl2	5′-GTGGATGACTGAGTACCT-3′	5′-CCAGGAGAAATCAAACAGAG-3′
Cdk5	5′-GCCAGACTATAAGCCCTACCC-3′	5′-GCTGCACAGGGTTACACTTC-3′
Mapt	5′-TCCAACTGCTGAAGACGTGA-3′	5′-CTTCTGGGATCTCCGTGTGG-3′
Gapdh	5′-CCGGGGTCCCAGCTTAGGTTCA-3′	5′-CGGCCAAATCCGTTCACACCGA-3′

Akt1, AKT-serine/threonine kinase 1; *Gfap*, glial fibrillary acidic protein; *Casp3*, caspase 3, apoptosis-associated cysteine peptidase; *Bax*, the Bcl-2 protein family, BCL2 associated X protein; *Bcl2*, B-cell lymphoma 2; *Cdk5*, cyclin-dependent kinase 5; *Mapt*, microtubule-associated protein tau; *Gapdh*, glyceraldehyde-3-phosphate dehydrogenase.

compared to P301S mice without isoD7-Aβ administration. Significant differences were observed only at the first time point: the number of exits to the arena periphery (p = 0.0125) and the average animal activity (p = 0.0089) were higher than in the P301S group without amyloid load. The C57Black6/J wild-type group maintained consistently high levels of speed, distance, and maximum time spent in the center of the arena throughout the experiment, indicating a low level of anxiety and preserved exploratory behavior (Figs. 3,4).

When assessing cognitive functions in the "Novel Object Recognition" test, a similar trend was observed in C57Black6/J mice: at both time points, this group demonstrated maximal values for speed, distance, as well as pref-

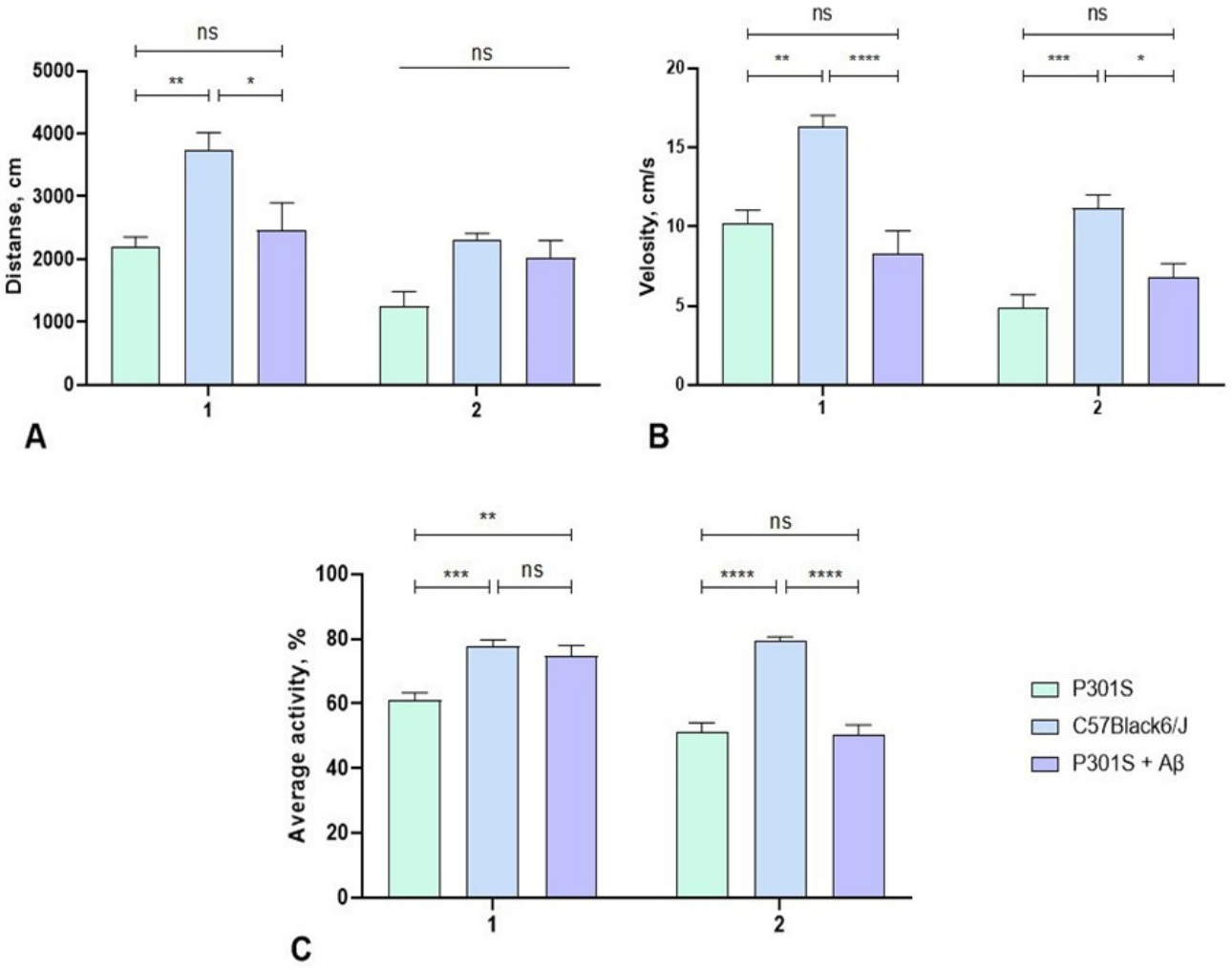

Fig. 3. Open field test. (A) distance traveled (cm), (B) velocity (cm/s), and (C) average activity (%). 1, first time point (16 weeks of age); 2, second time point (20 weeks of age). n = 10, biological duplication. ns, not significant; * $p \leq 0.05$; ** $p \leq 0.01$; *** $p \leq 0.001$; **** $p \leq 0.0001$.

erence and discrimination indices, which were statistically significantly higher than the corresponding indicators in mice with tauopathy. This confirms the preserved ability for novel object recognition in wild-type animals. In contrast, the experimental P301S+Aβ group and the control P301S group without amyloid load showed comparably low indicators characterizing cognitive functions at both time points. No statistically significant differences were found between the P301S+Aβ and P301S groups without isoD7-Aβ administration in the main analyzed parameters. At the second time point, the level of preference in the P301S+Aβ group was statistically lower than in the C57Black6/J mice ($p = 0.0301$); a similar trend was observed for the discrimination index ($p < 0.0001$) (Fig. 5).

More pronounced differences between groups were observed in the motor coordination tests. In the "Vertical Pole" test, at the first time point, mice in the P301S+Aβ group required less time to turn on the vertical pole compared to the control P301S group without amyloid load ($p = 0.0432$), whereas at the second time point, this indicator was comparable between the groups. This suggests an earlier development of motor impairments in the P301S+Aβ group compared to P301S mice without additional amyloid load. However, the total time spent on the vertical pole at both time points did not differ statistically significantly between the tauopathy groups (Fig. 6).

A similar trend was observed in the "Inverted Screen" test: 16-week-old P301S+Aβ mice held onto the screen for a shorter duration compared to the control P301S group without amyloid load ($p = 0.0316$). At the second time point, no statistically significant differences were found between these groups (Fig. 7).

3.2 Results of Immunohistochemical and Histological Studies

Immunohistochemical examination of brain sections from 24-week-old mice revealed that in the P301S+Aβ group, the number of neurons with positive AT-8 im-

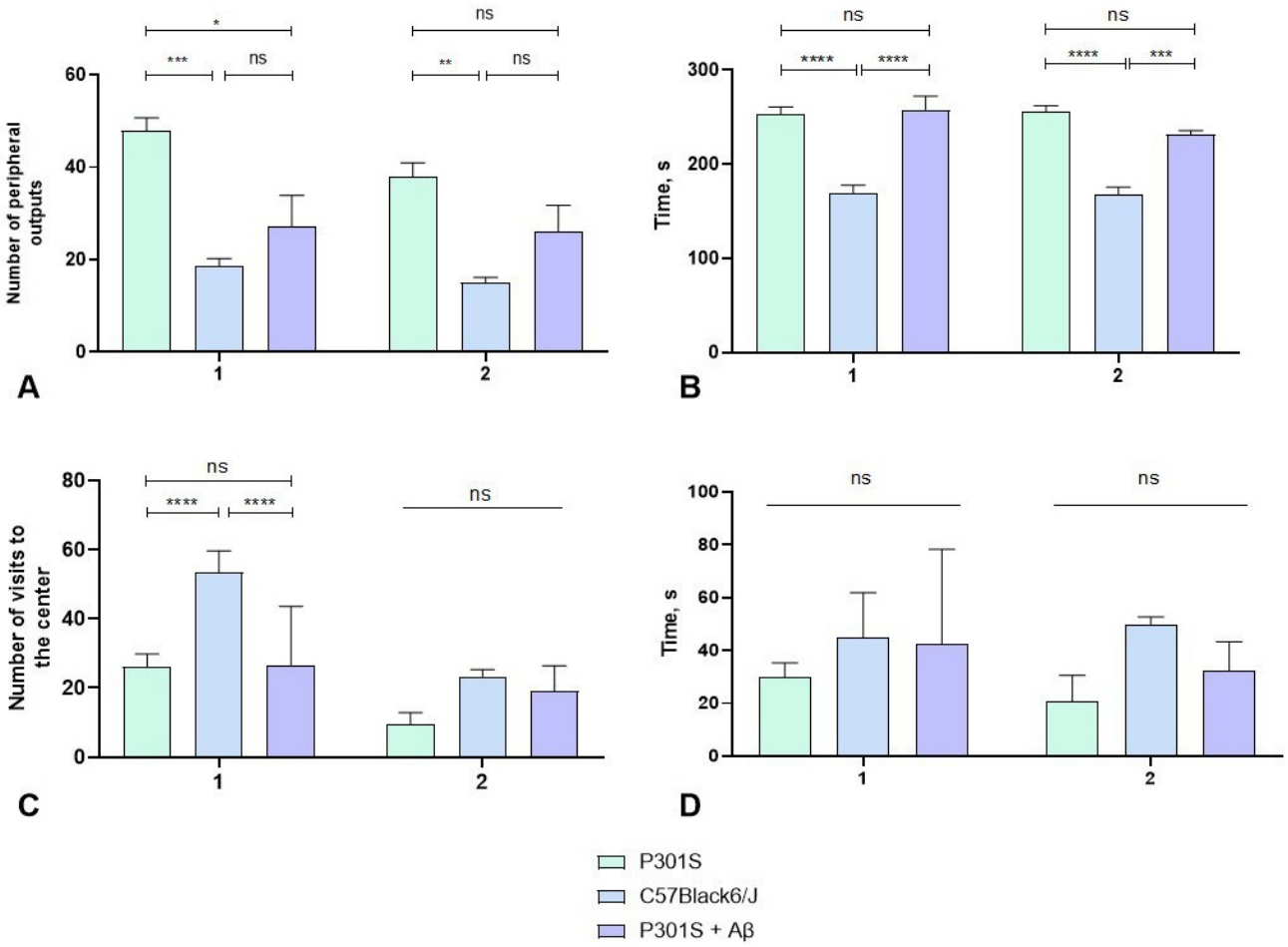

Fig. 4. Open field test. (A) number of entries into the peripheral zone, (B) time spent in the peripheral zone (s), (C) number of entries into the center, and (D) time spent in the center (s). 1, first time point (16 weeks of age); 2, second time point (20 weeks of age). n = 10. ns, not significant; * $p \leq 0.05$; ** $p \leq 0.01$; *** $p \leq 0.001$; **** $p \leq 0.0001$.

munostaining in the brainstem was statistically significantly higher than in the control P301S group without amyloid load ($p = 0.0344$). No statistically significant differences were found in the frontal cortex between these groups. In C57Black6/J wild-type mice, neurons with positive AT-8 immunostaining were absent in the studied structures (Figs. 8,9).

Histological examination of brain sections from 24-week-old mice revealed no Congo red-positive amyloid deposits in the brain regions examined (entorhinal cortex and hippocampus) (Fig. 10).

3.3 Relative Normalized Quantitative Analysis of Gene Expression Results

Gene expression levels in the frontal cortex of 24-week-old mice were assessed semiquantitatively by real-time PCR (qRT-PCR) with normalization to the reference gene Gapdh using the $2^{-\Delta Ct}$ formula (Fig. 11). Data are presented as mean ± standard deviation (mean ± SD); differences were considered statistically significant at $p < 0.05$. A total of seven target genes were analyzed with two types of comparisons: P301S+Aβ vs P301S and P301S+Aβ vs C57Black6/J.

Akt1 gene expression in the P301S+Aβ group (0.421 ± 0.091) was significantly reduced compared to both the P301S control group (1.045 ± 0.102, $p < 0.01$) and wild-type C57Black6/J mice (0.978 ± 0.110, $p < 0.01$), indicating a significant impairment of *PI3K/Akt* signaling following peripheral administration of isoD7-Aβ. The expression level of *Gfap*, a marker of astrogliosis, was significantly higher in the P301S+Aβ group (1.949 ± 0.208) than in control P301S mice (0.938 ± 0.229, $p < 0.01$) and C57Black6/J mice (0.540 ± 0.141, $p < 0.001$), indicating an enhanced neuroinflammatory response with isoD7-Aβ administration. The expression of *Casp3* in the P301S+Aβ group (0.050 ± 0.023) was not significantly different from either the control P301S group (0.019 ± 0.009, $p = 0.808$) or C57Black6/J mice (0.011 ± 0.010, $p = 0.695$). However, a trend toward increased *Casp3* levels was observed in the isoD7-Aβ-treated group.

Expression of the pro-apoptotic gene *Bax* in the P301S+Aβ group (0.995 ± 0.087) was significantly higher

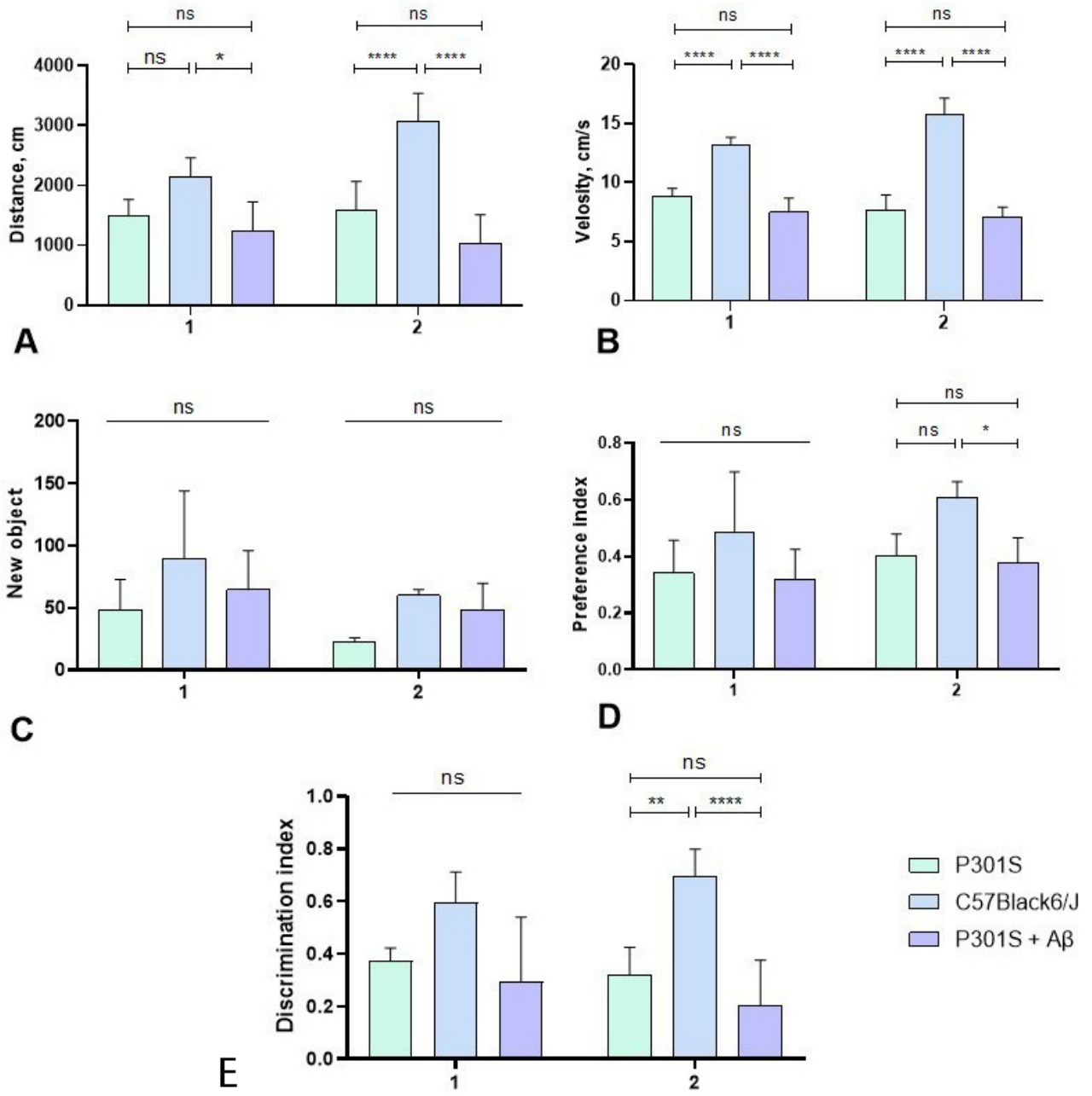

Fig. 5. Novel object recognition test. (A) distance traveled (cm), (B) velocity (cm/s), (C) exploration of the novel object [or actual parameter name], (D) preference index, and (E) discrimination index. 1, first time point (16 weeks of age); 2, second time point (20 weeks of age). n = 10. ns, not significant; * $p \leq 0.05$; ** $p \leq 0.01$; **** $p \leq 0.0001$.

than in control P301S mice (0.585 ± 0.065, $p < 0.01$) and C57Black6/J mice (0.514 ± 0.120, $p < 0.05$), reflecting an increase in the pro-apoptotic signal under the influence of isoD7-Aβ.

The expression level of the anti-apoptotic gene *Bcl2* in the P301S+Aβ group (0.470 ± 0.100) was significantly lower than in control P301S mice (0.907 ± 0.11, $p < 0.05$) and C57Black6/J mice (0.994 ± 0.098, $p < 0.05$). Thus, the introduction of isoD7-Aβ was accompanied by a shift in the balance of apoptotic gene expression towards the pro-apoptotic side.

Cdk5 expression in the P301S+Aβ group (1.032 ± 0.097) was not statistically different from either control P301S mice (1.015 ± 0.086, $p = 0.931$) or C57Black6/J mice (1.036 ± 0.109, $p = 0.997$).

Mapt expression in the P301S+Aβ group (1.962 ± 0.141) was not statistically different from control P301S mice (1.954 ± 0.160, $p = 0.983$), but was significantly higher than in wild-type C57Black6/J mice (0.249 ± 0.243, $p < 0.001$). This confirms that isoD7-Aβ administration does not affect transcription of the *Mapt* gene itself, but is associated with increased post-translational tau pathology.

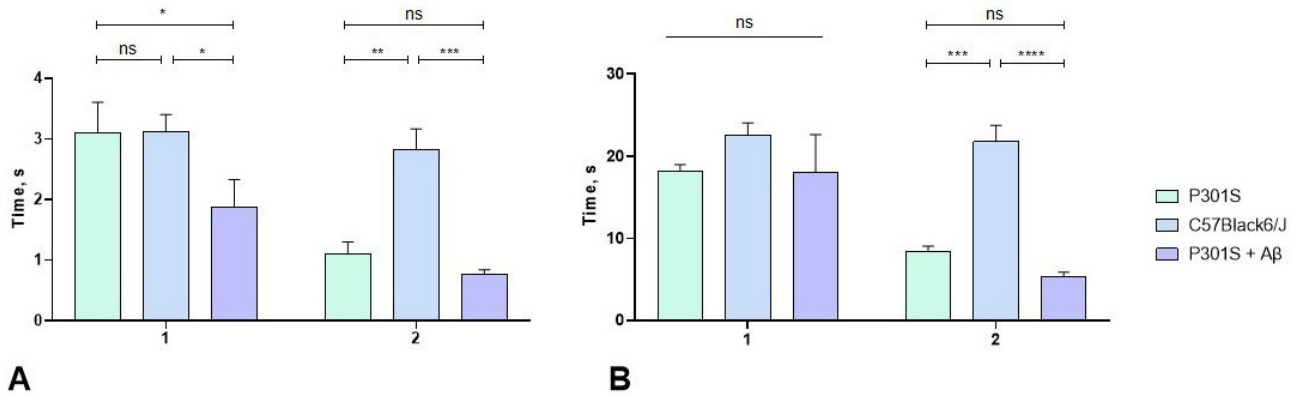

Fig. 6. Vertical pole test. (A) turning time (s) and (B) total time on the pole (s). 1, first time point (16 weeks of age); 2, second time point (20 weeks of age). n = 10. ns, not significant; * $p \leq 0.05$; ** $p \leq 0.01$; *** $p \leq 0.001$; **** $p \leq 0.0001$.

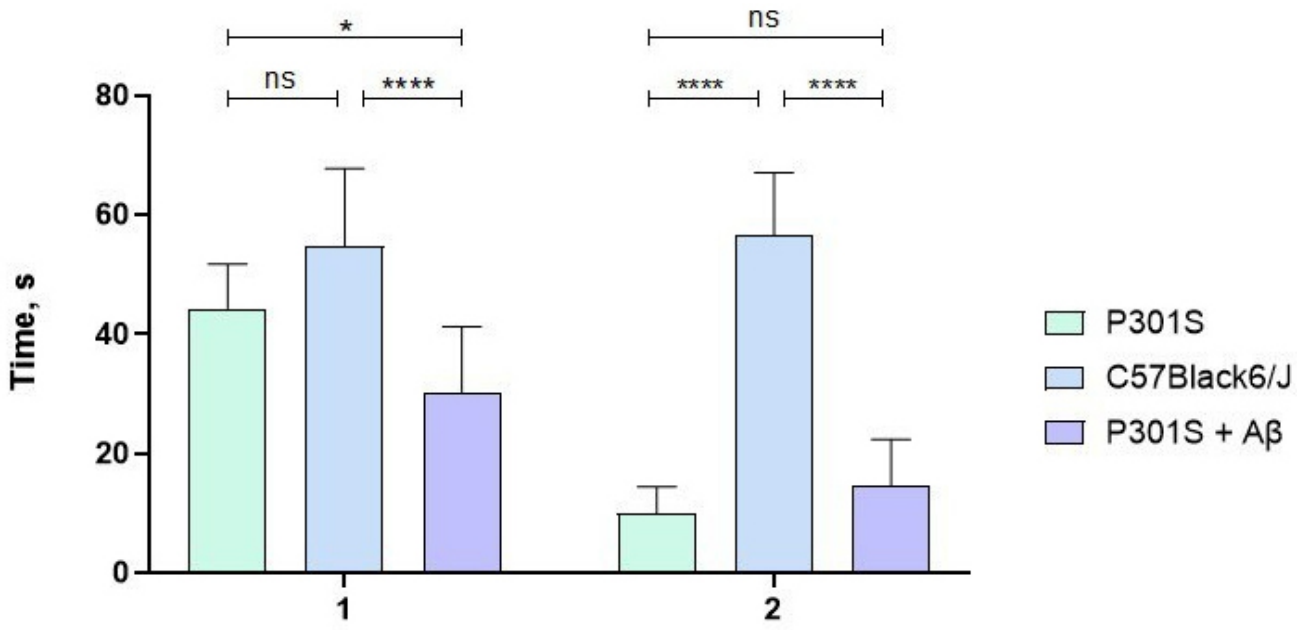

Fig. 7. Inverted screen test. Retention time on the inverted screen (s). 1, first time point (16 weeks of age); 2, second time point (20 weeks of age). n = 10. ns, not significant; * $p \leq 0.05$; **** $p \leq 0.0001$.

4. Discussion

Alzheimer's disease is characterized by two key pathological hallmarks: extracellular accumulation of Aβ and intracellular aggregation of hyperphosphorylated tau protein [17]. Currently, increasing evidence points to a synergism between Aβ and tau pathology: the presence of Aβ can accelerate tau phosphorylation and spreading in various experimental models. This suggests that the observed effects are not associated with the development of classical amyloid plaque pathology, but may instead reflect the action of soluble amyloid species or the activation of peripheral-to-central signaling mechanisms. Therefore, the present data do not allow us to distinguish whether the observed effects reflect direct brain entry of the administered peptide, actions of soluble peripheral amyloid species, or indirect peripheral-to-central signaling mechanisms, including inflammatory or vascular pathways [18,19,20,21,22,23]. However, the question of whether peripherally administered Aβ is able to modulate pre-existing tau pathology in the CNS without direct intracranial action remains poorly understood. The clinical relevance of this question is further supported by evidence of impaired Aβ transport across the blood–brain barrier in AD, including an altered balance between its entry into the brain and clearance from the brain [24,25]. The study was conducted exclusively on male transgenic mice of the P301S line, since based on previously published data from Anthony M Downs et al., 2025 [26], it was found that male and female changes in the experiment did not depend on gender in relation to the obtained electrophysiological properties of neurons (decreased excitatory inputs and kinetics of excitatory postsynaptic current). And in a study conducted by Denise

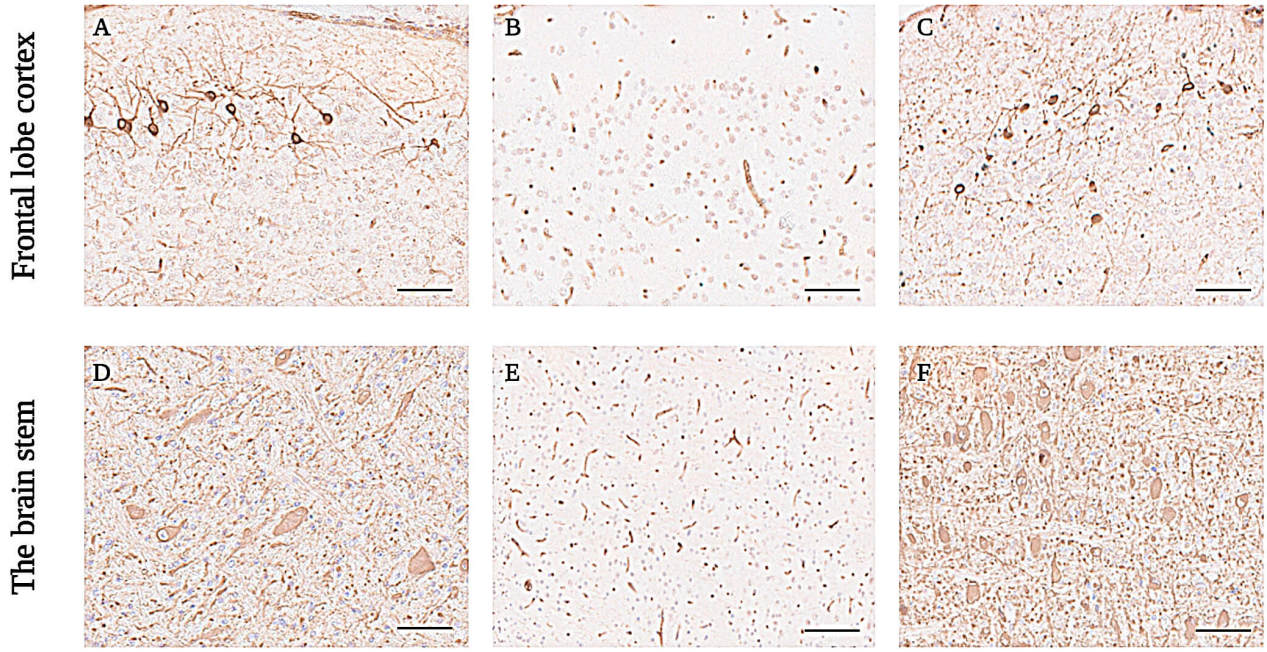

Fig. 8. Representative AT-8-immunostained sections of the frontal cortex and brainstem. (A,D) control P301S mice, (B,E) C57Black6/J wild-type mice, and (C,F) P301S+Aβ mice. Scale bar = 200 μm.

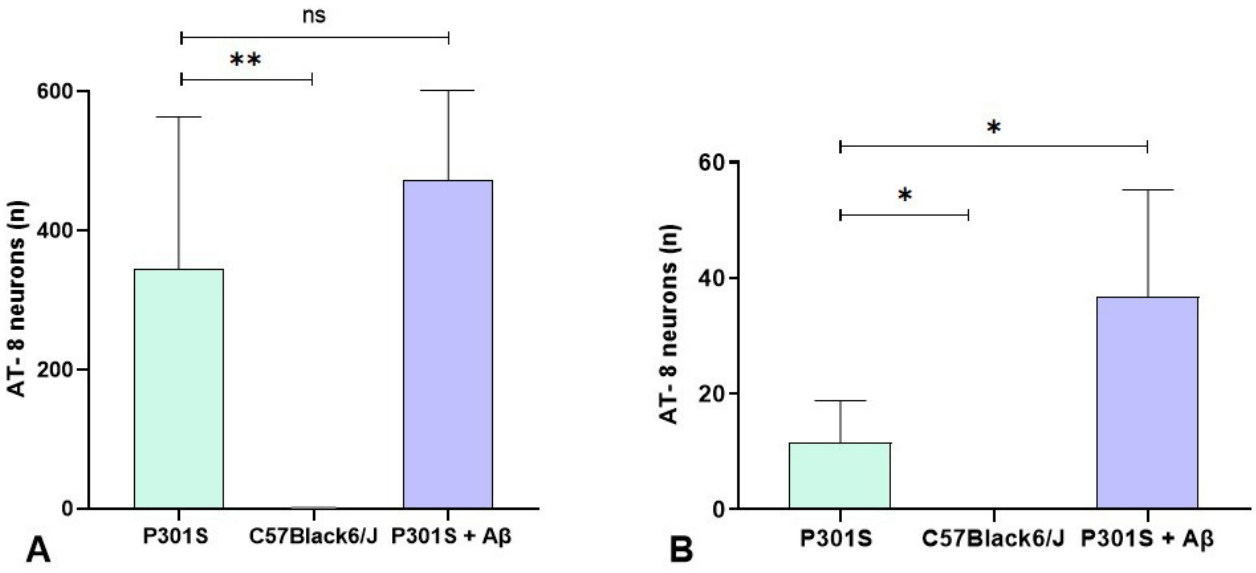

Fig. 9. The number of AT-8-immunostained neurons in the P301S+Aβ group relative to the P301S control. Histogram showing an increased number of AT-8 immunostained neurons in the P301S+Aβ group compared to the control P301S group; where (A) – frontal cortex, (B) – brainstem; ns – no statistically significant differences; * $p \leq 0.05$, ** $p \leq 0.01$.

M.O. Ramirez and co-authors in 2025 [27], found no sex differences, since gender did not affect either the pathological tau protein or the structure of its accumulation at any age in this mouse model. In the present study, we demonstrated that double peripheral administration of isoD7-Aβ to P301S mice was associated with earlier development of motor impairments and increased AT-8-positive tau pathology, primarily in the brainstem. However, no additional impairment in open-field and novel object recognition tests was observed compared to the P301S control group. This suggests that, at this stage of the model, peripheral amyloid burden has a greater impact on structures associated with motor control than on cognitive functions, which are already impaired in animals of this line [28,29,30]. The choice of the

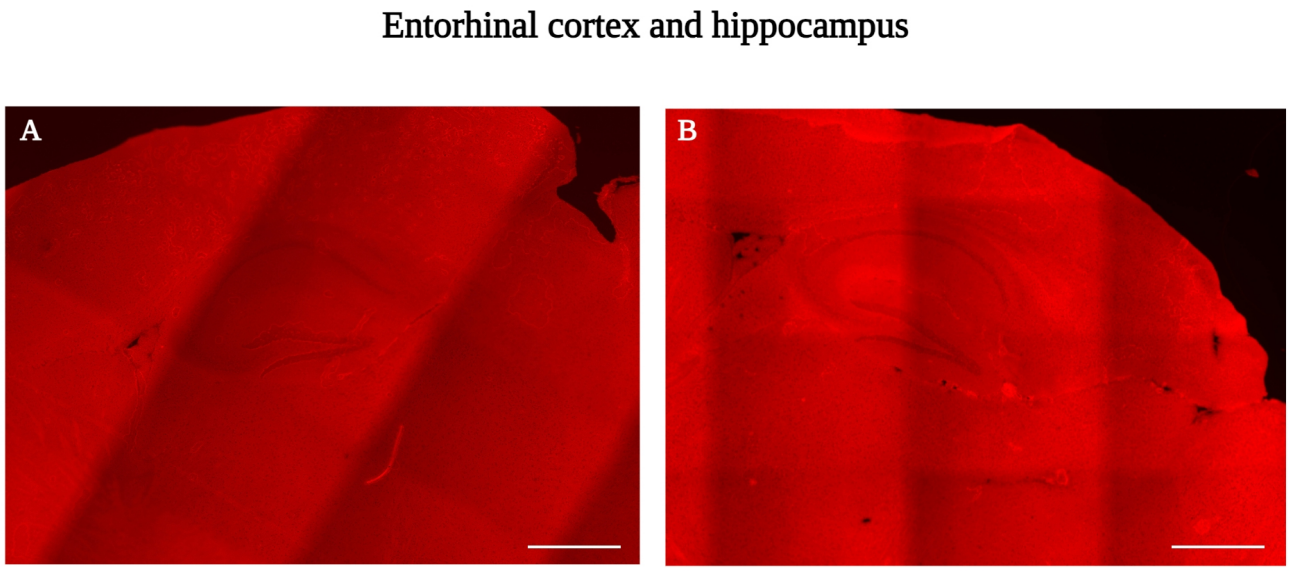

Fig. 10. Representative Congo red-stained sections of the entorhinal cortex and hippocampus from (A) control P301S mice and (B) P301S+Aβ mice. Histological examination of brain sections from 24-week-old mice revealed no Congo red-positive amyloid deposits in the entorhinal cortex or hippocampus under bright-field microscopy. Scale bar = 40 μm.

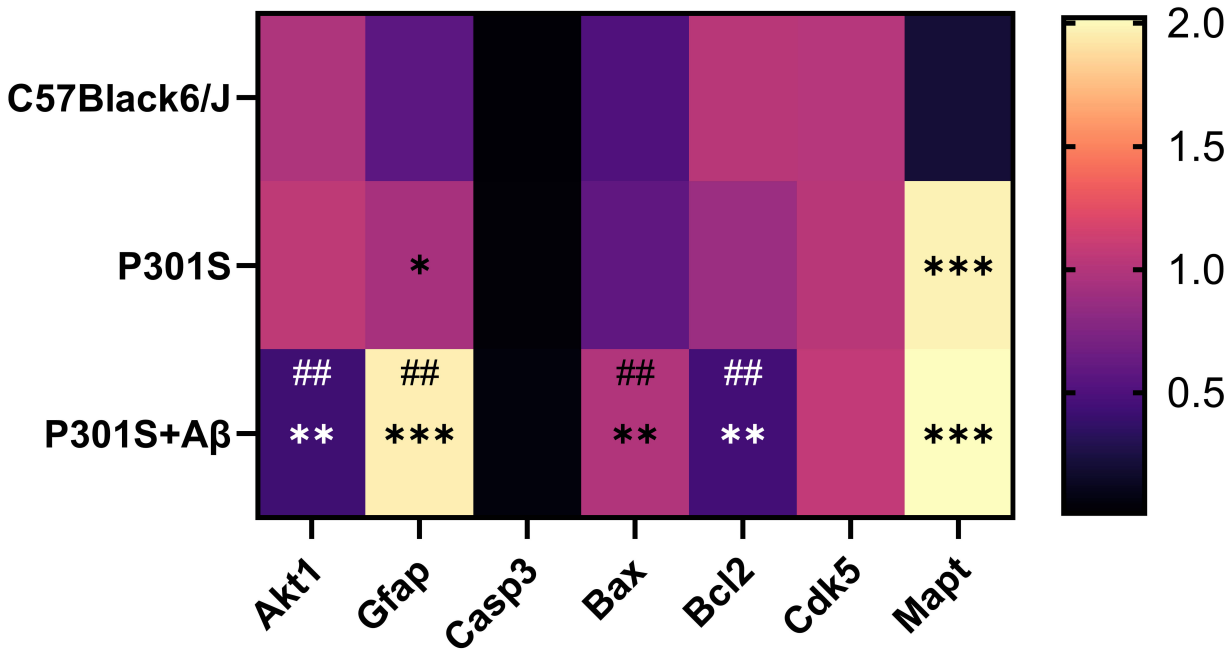

Fig. 11. Heat map of relative gene expression levels determined by qRT-PCR in the frontal cortex of mice. The table presents the mean relative gene expression values normalized to the reference gene Gapdh using the $2^{-\Delta Ct}$ formula for seven genes of interest (*Akt1, Gfap, Casp3, Bax, Bcl2, Cdk5,* and *Mapt*) in two groups of mice with tauopathy: control (P301S) and with retroorbital injection of isoD7-Aβ (P301S + Aβ); in comparison with wild-type C57Black6/J mice (genetic background). Double peripheral administration of isoD7-Aβ to P301S mice is accompanied by molecular changes consistent with possible involvement of the Akt/GSK-3β-associated pathway, namely, decreased *Akt1*, increased *Gfap, Bax*, and decreased *Bcl2,* with no significant effects on *Cdk5* and *Mapt*. The color scale indicates the relative expression level, where dark blue (0.5 and below) means the expression level is very low relative to the housekeeping gene Gapdh, shades from pink to bright yellow (1.0 and above) mean the expression level is moderately higher or much higher relative to the housekeeping gene Gapdh. Asterisks mark the values of statistical significance of the difference between the experimental and comparison (WT) groups — * ($p < 0.05$), ** ($p < 0.01$), *** ($p < 0.001$). Pound signs mark the statistical significance of the difference between the experimental groups (P301S + Aβ vs P301S) – ## ($p < 0.01$).

isomerized form of Aβ is crucial. According to the literature, isoD7-Aβ exhibits more pronounced neurotoxic properties compared to native Aβ [31] and is capable of modulating amyloidogenesis *in vivo* [32,33]. Furthermore, isoD7-Aβ has been shown to induce higher levels of protein phosphorylation, including tau protein, in SH-SY5Y neuroblastoma cells [14]. In this context, our results complement existing concepts and indicate that peripherally administered isoD7-Aβ can enhance the manifestations of tau pathology *in vivo* against the background of pre-existing tauopathy.

An important observation is the absence of Congo red-positive amyloid deposits in the studied brain regions. This suggests that the observed effects are not associated with the development of classical amyloid plaque pathology, but may be due to either the effect of soluble amyloid forms or the activation of peripheral-central signaling mechanisms. This interpretation is consistent with data on the role of the systemic Aβ pool, impaired blood-brain barrier function, and the possible involvement of vascular and transport mechanisms in the maintenance of cerebral pathology [24,25].

Molecular results are also consistent with the proposed pathogenetic scheme. In the P301S+Aβ group, decreased Akt1 expression, increased Gfap and Bax expression, and a decrease in Bcl2 were detected. Taken together, these changes correspond to a profile that may reflect impaired PI3K/Akt regulation, increased glial activation, and a pro-apoptotic shift [11]. The absence of significant changes in Cdk5 and Mapt expression makes it less likely that alternative mechanisms associated with increased transcription of the tau protein itself or pronounced involvement of the Cdk5-dependent pathway are involved [34]. The data on Casp3 were not statistically significant and should therefore be interpreted with caution [11].

The obtained data are generally consistent with the idea that even a short-term increase in the amyloid signal can have a long-term impact on the course of tau pathology. This is consistent with the results of Selenica et al. [23], who showed that chronic exposure to Aβ potentiates tau pathology in the rTg4510 model, and changes in p-tau and GSK-3β activity can persist even after cessation of Aβ administration. A similar phenomenon of long-term persistence of pathological changes after modification of the amyloid cascade has been discussed in a clinical context [34]. Although our study did not directly assess the irreversibility of the changes, the persistence of effects several weeks after double exposure may indicate the persistent nature of the induced pathological shifts.

Thus, the combination of behavioral, immunohistochemical, and transcriptional data supports the hypothesis that peripheral amyloid burden can potentiate the course of tauopathy. The obtained results also confirm the feasibility of using peripheral administration of modified forms of Aβ, including isoD7-Aβ, as an experimental approach for modeling "amyloid-associated signaling load" in the presence of pre-existing tau pathology. This approach allows us to study the interaction of Aβ and tau components of neurodegeneration without creating complex dual transgenic models [3].

From a therapeutic perspective, the results support the relevance of combined interventions targeting the amyloid and tau components of AD pathogenesis [3]. Despite the introduction of anti-amyloid drugs into clinical practice, their effect remains limited [6,7]. This indicates the need to search for additional therapeutic targets and combined approaches aimed at both the amyloid and tau components of pathogenesis [3,8]. In this context, the Akt/GSK-3β-associated signaling pathway is of particular interest, as it lies at the intersection of processes associated with amyloid toxicity, tau phosphorylation, neuroinflammation, and apoptosis [11].

When interpreting the results, it is necessary to consider the limitations of the study. First, transcriptional analysis does not provide direct evidence of changes in GSK-3β activity, so the putative involvement of the Akt/GSK-3β-associated signaling pathway is indirect [11,35]. Second, the study did not evaluate the distribution and accumulation of exogenous isoD7-Aβ itself in brain tissue, leaving the question of the ratio of direct and indirect mechanisms of action open [22,23]. Third, the double administration regimen used does not allow one to assess the cumulative effects of chronic amyloid stimulation. Nevertheless, the obtained results indicate the potential of this model for further study of the mechanisms of Aβ–tau interaction and the search for combined therapeutic strategies [3,11].

5. Conclusion

The study demonstrated that double peripheral administration of isoD7-Aβ to P301S mice was associated with earlier development of motor impairment and increased AT-8-positive tau pathology. Molecular analysis revealed changes in gene expression consistent with disruption of the Akt/GSK-3β-associated signaling pathway, increased glial activation, and the formation of a proapoptotic shift. The persistence of these effects several weeks after double administration may indicate the persistent nature of the induced pathological changes.

These results support the hypothesis of synergism between Aβ and tau in the pathogenesis of neurodegenerative diseases, as well as the concept of interaction between amyloid and tau components in the neurodegenerative process. Furthermore, they indicate the possible involvement of the Akt/GSK-3β-associated signaling pathway, which requires further direct experimental verification. The model of peripheral administration of modified Aβ in the setting of genetically determined tauopathy represents a valuable experimental approach to study the mechanisms of interaction between these two pathological processes and to test combination therapeutic strategies directed at multiple molecular targets.

Availability of Data and Materials

The datasets used and analyzed during the current study are available from the corresponding author on reasonable request.

Author Contributions

YS — author participated in the study design, conducted the experimental work, analyzed the data, and contributed to the writing of the article. OS — author performed a comprehensive analysis of the collected data and developed the study methodology. NZ — author performed the quantitative gene expression analysis, interpreted the data, and contributed to the drafting of the manuscript. VS — author analyzed the results and contributed to all aspects of the experimental work and the writing of the article. SK — author analyzed the results obtained at all stages of the study and contributed to editing the final version of the publication. VM — author analyzed the results obtained at all stages of the study and contributed to editing the final version of the publication. AR — author contributed to the writing of the article and the interpretation of the results obtained in the behavioral testing block. EK — performed histological staining, analyzed the results, and contributed to the article. LK — author contributed to the writing of the article and the interpretation of the results obtained in the behavioral testing block. MK — developed the study design, supervised immunohistochemical staining of the sections, and oversaw all stages of the study. All authors contributed to editorial changes in the manuscript. All authors read and approved the final manuscript. All authors have participated sufficiently in the work and agreed to be accountable for all aspects of the work.

Ethics Approval and Consent to Participate

The experiments and animal manipulations were approved by the Bioethics Committee of Belgorod State National Research University (No. 03-01i/25 dated September 1, 2025) and the ARRIVE guidelines (see **Supplementary Material**, item 8b). The study complied with the requirements of Directive 2010/63/EU of the European Parliament and of the Council on the protection of animals used for scientific purposes, as well as the national standard of the Russian Federation GOST 33044-2014 “Principles of Good Laboratory Practice” (GLP).

Acknowledgment

The graphic abstract was drawn using BioRender software (https://www.biorender.com/). Pokrovkiy, V. (2026) https://BioRender.com/nrecwwj.

Funding

This research was funded by the Program of Fundamental Research in the Russian Federation (projects # FZWG-2026-0003 and 124031800075-1).

Conflicts of Interest

The authors declare no conflicts of interest.

Supplementary Material

Supplementary material associated with this article can be found, in the online version, at https://doi.org/10.31083/FBL53279.

References

[1] World Health Organization. Dementia. 2021. Available at: https://www.who.int/news-room/facts-in-pictures/detail/dementia (Accessed: 16 January 2026).

[2] Liu W, Deng W, Gong X, Ou J, Yu S, Chen S. Global burden of Alzheimer’s disease and other dementias in adults aged 65 years and over, and health inequality related to SDI, 1990-2021: analysis of data from GBD 2021. BMC Public Health. 2025; 25: 1256. https://doi.org/10.1186/s12889-025-22378-z

[3] Busche MA, Hyman BT. Synergy between amyloid-β and tau in Alzheimer’s disease. Nature Neuroscience. 2020; 23: 1183–1193. https://doi.org/10.1038/s41593-020-0687-6

[4] Holmes C, Boche D, Wilkinson D, Yadegarfar G, Hopkins V, Bayer A, et al. Long-term effects of Abeta42 immunisation in Alzheimer’s disease: follow-up of a randomised, placebo-controlled phase I trial. Lancet (London, England). 2008; 372: 216–223. https://doi.org/10.1016/S0140-6736(08)61075-2

[5] Aisen PS, Gauthier S, Ferris SH, Saumier D, Haine D, Garceau D, et al. Tramiprosate in mild-to-moderate Alzheimer’s disease - a randomized, double-blind, placebo-controlled, multi-centre study (the Alphase Study). Archives of Medical Science: AMS. 2011; 7: 102–111. https://doi.org/10.5114/aoms.2011.20612

[6] Jiang X, Lv G, Mendes ME, Wu J, Yuan J, Lu ZK. Lifetime cost-effectiveness of lecanemab for early Alzheimer’s disease. Frontiers in Public Health. 2026; 14: 1692508. https://doi.org/10.3389/fpubh.2026.1692508

[7] Herrup K. The case for rejecting the amyloid cascade hypothesis. Nature Neuroscience. 2015; 18: 794–799. https://doi.org/10.1038/nn.4017

[8] Di J, Siddique I, Li Z, Malki G, Hornung S, Dutta S, et al. The molecular tweezer CLR01 improves behavioral deficits and reduces tau pathology in P301S-tau transgenic mice. Alzheimer’s Research & Therapy. 2021; 13: 6. https://doi.org/10.1186/s13195-020-00743-x

[9] Garbuz DG, Zatsepina OG, Evgen’ev MB. Beta Amyloid, Tau Protein, and Neuroinflammation: An Attempt to Integrate Different Hypotheses of Alzheimer’s Disease Pathogenesis. Molekuliarnaia Biologiia. 2021; 55: 734–747. https://doi.org/10.31857/S0026898421050049

[10] Shin WS, Di J, Cao Q, Li B, Seidler PM, Murray KA, et al. Amyloid β-protein oligomers promote the uptake of tau fibril seeds potentiating intracellular tau aggregation. Alzheimer’s Research & Therapy. 2019; 11: 86. https://doi.org/10.1186/s13195-019-0541-9

[11] Limantoro J, de Liyis BG, Sutedja JC. Akt signaling pathway: a potential therapy for Alzheimer’s disease through glycogen synthase kinase 3 beta inhibition. The Egyptian Journal of Neurology, Psychiatry and Neurosurgery. 2023; 59: 147. https://doi.org/10.1186/s41983-023-00751-2

[12] Mitkevich VA, Petrushanko IY, Yegorov YE, Simonenko OV, Vishnyakova KS, Kulikova AA, et al. Isomerization of Asp7 leads to increased toxic effect of amyloid-β42 on human neuronal cells. Cell Death & Disease. 2013; 4: e939. https://doi.org/10.1038/cddis.2013.492

[13] Moro ML, Phillips AS, Gaimster K, Paul C, Mudher A, Nicoll JAR, et al. Pyroglutamate and Isoaspartate modified Amyloid-

Beta in ageing and Alzheimer's disease. Acta Neuropathologica Communications. 2018; 6: 3. https://doi.org/10.1186/s40478-017-0505-x

[14] Zatsepina OG, Kechko OI, Mitkevich VA, Kozin SA, Yurinskaya MM, Vinokurov MG, et al. Amyloid-β with isomerized Asp7 cytotoxicity is coupled to protein phosphorylation. Scientific Reports. 2018; 8: 3518. https://doi.org/10.1038/s41598-018-21815-x

[15] Kumar S, Rezaei-Ghaleh N, Terwel D, Thal DR, Richard M, Hoch M, et al. Extracellular phosphorylation of the amyloid β-peptide promotes formation of toxic aggregates during the pathogenesis of Alzheimer's disease. The EMBO Journal. 2011; 30: 2255–2265. https://doi.org/10.1038/emboj.2011.138

[16] Fukuda H, Shimizu T, Nakajima M, Mori H, Shirasawa T. Synthesis, aggregation, and neurotoxicity of the Alzheimer's Abeta1-42 amyloid peptide and its isoaspartyl isomers. Bioorganic & Medicinal Chemistry Letters. 1999; 9: 953–956. https://doi.org/10.1016/s0960-894x(99)00121-3

[17] Zhang J, Zhang Y, Wang J, Xia Y, Zhang J, Chen L. Recent advances in Alzheimer's disease: Mechanisms, clinical trials and new drug development strategies. Signal Transduction and Targeted Therapy. 2024; 9: 211. https://doi.org/10.1038/s41392-024-01911-3

[18] Kozin SA, Cheglakov IB, Ovsepyan AA, Telegin GB, Tsvetkov PO, Lisitsa AV, et al. Peripherally applied synthetic peptide isoAsp7-Aβ(1-42) triggers cerebral β-amyloidosis. Neurotoxicity Research. 2013; 24: 370–376. https://doi.org/10.1007/s12640-013-9399-y

[19] Morito T, Qi M, Kamano N, Sasaguri H, Bez S, Foiani M, et al. Human MAPT knockin mouse models of frontotemporal dementia for the neurodegenerative research community. Cell Reports Methods. 2025; 5: 101024. https://doi.org/10.1016/j.crmeth.2025.101024

[20] Welikovitch LA, Mate de Gerando A, Khasnavis A, Bhavsar H, Meltzer JC, Buée L, et al. Tau, synapse loss and gliosis progress in an Alzheimer's mouse model after amyloid-β immunotherapy. Brain: a Journal of Neurology. 2025; 148: 1316–1328. https://doi.org/10.1093/brain/awae345

[21] Han YE, Lim S, Lee SE, Nam MH, Oh SJ. Novel mouse model of Alzheimer's disease exhibits pathology through synergistic interactions among amyloid-β, tau, and reactive astrogliosis. Zoological Research. 2025; 46: 41–53. https://doi.org/10.24272/j.issn.2095-8137.2024.257

[22] Götz J, Chen F, van Dorpe J, Nitsch RM. Formation of neurofibrillary tangles in P301l tau transgenic mice induced by Abeta 42 fibrils. Science (New York, N.Y.). 2001; 293: 1491–1495. https://doi.org/10.1126/science.1062097

[23] Selenica MLB, Brownlow M, Jimenez JP, Lee DC, Pena G, Dickey CA, et al. Amyloid oligomers exacerbate tau pathology in a mouse model of tauopathy. Neuro-degenerative Diseases. 2013; 11: 165–181. https://doi.org/10.1159/000337230

[24] Donahue JE, Flaherty SL, Johanson CE, Duncan JA, 3rd, Silverberg GD, Miller MC, et al. RAGE, LRP-1, and amyloid-beta protein in Alzheimer's disease. Acta Neuropathologica. 2006; 112: 405–415. https://doi.org/10.1007/s00401-006-0115-3

[25] Deng Y, Yin H, Lu Z, Lan H, Liu W, Zuo C, et al. LRP1 at the crossroads of Aβ clearance and therapeutic targeting in Alzheimer's disease. Frontiers in Aging Neuroscience. 2026; 17: 1669405. https://doi.org/10.3389/fnagi.2025.1669405

[26] Downs AM, Kmiec G, Catavero CM, Wykoff LA, McElligott ZA. Loss of excitatory inputs and decreased tonic and evoked activity of locus coeruleus neurons in aged P301S mice. Neurobiology of Disease. 2025; 208: 106883. https://doi.org/10.1016/j.nbd.2025.106883

[27] Ramirez DMO, Whitesell JD, Bhagwat N, Thomas TL, Ajay AD, Nawaby A, et al. Spontaneous pathology in PS19 tauopathy mice progresses via brain networks. Neurobiology of Disease. 2025; 215: 107072. https://doi.org/10.1016/j.nbd.2025.107072

[28] Stepenko YV, Shmigerova VS, Kostina DA, Shcheblykina OV, Zhernakova NI, Solin AV, Koroleva NV, Markovskaya VA, Dudnikova OV, Bolgov AA. Study of the neuroprotective properties of the heteroreceptor EPOR/CD131 agonist of peptide structure in tau proteinopathy modeling. Research Results in Pharmacology. 2024; 10: 41–47.

[29] Shmigerova VS, Stepenko YuV, Kurbatova AA, Zhunusov NS, Lyapkalov NS, Sviridova MS, et al. Investigation of the pharmacological activity of the tetrapeptide HAEE, zinc, and human serum albumin in a transgenic mouse model with tau protein overexpression (P301S). Research Results in Pharmacology. 2025; 11: 49–57.

[30] Dumont M, Stack C, Elipenahli C, Jainuddin S, Gerges M, Starkova NN, et al. Behavioral deficit, oxidative stress, and mitochondrial dysfunction precede tau pathology in P301S transgenic mice. FASEB Journal: Official Publication of the Federation of American Societies for Experimental Biology. 2011; 25: 4063–4072. https://doi.org/10.1096/fj.11-186650

[31] Barykin EP, Garifulina AI, Kruykova EV, Spirova EN, Anashkina AA, Adzhubei AA, et al. Isomerization of Asp7 in Beta-Amyloid Enhances Inhibition of the α7 Nicotinic Receptor and Promotes Neurotoxicity. Cells. 2019; 8: 771. https://doi.org/10.3390/cells8080771

[32] Kozin SA, Barykin EP, Telegin GB, Chernov AS, Adzhubei AA, Radko SP, et al. Intravenously Injected Amyloid-β Peptide With Isomerized Asp7 and Phosphorylated Ser8 Residues Inhibits Cerebral β-Amyloidosis in AβPP/PS1 Transgenic Mice Model of Alzheimer's Disease. Frontiers in Neuroscience. 2018; 12: 518. https://doi.org/10.3389/fnins.2018.00518

[33] Nicoll JAR, Buckland GR, Harrison CH, Page A, Harris S, Love S, et al. Persistent neuropathological effects 14 years following amyloid-β immunization in Alzheimer's disease. Brain: a Journal of Neurology. 2019; 142: 2113–2126. https://doi.org/10.1093/brain/awz142

[34] Baltissen D, Bold CS, Rehra L, Banićević M, Fricke J, Just J, et al. APPsα rescues CDK5 and GSK3β dysregulation and restores normal spine density in Tau transgenic mice. Frontiers in Cellular Neuroscience. 2023; 17: 1106176. https://doi.org/10.3389/fncel.2023.1106176

[35] Rankin CA, Sun Q, Gamblin TC. Tau phosphorylation by GSK-3beta promotes tangle-like filament morphology. Molecular Neurodegeneration. 2007; 2: 12. https://doi.org/10.1186/1750-1326-2-12